

Cite this: *Org. Biomol. Chem.*, 2023, **21**, 514Received 27th October 2022,
Accepted 6th December 2022

DOI: 10.1039/d2ob01965e

rsc.li/obc

Munronin V with 7/7/6 tricarbocyclic framework from *Munronia henryi* harms inhibits tau pathology by activating autophagy†

Ying Yan,^{‡a} Xiaoqian Ran,^{‡b,c} Dan Wang,^a Xiong Zhang,^a Mingyou Peng,^a Xiaoyan Yan,^a Lei Tang,^a Hong Liang,^d Xujie Qin,^d Ying-Tong Di,^{id d} Rongcan Luo,^{id *b,c} Xiao-Jiang Hao^{id *d} and Yong-Gang Yao^{id b,c,e}

Munronin V (1), isolated from *Munronia henryi* Harms, is the first example, to the best of our knowledge, of an unprecedented 7/7/6 tricarbocyclic framework featuring an unusual A,B-*seco*-limonoid ring. The structures of munronin V were established from extensive spectroscopic and electronic circular dichroism (ECD) analyses. The novel A,B-*seco* with two seven-membered lactones was formed as a result of Baeyer–Villiger oxidation. Compound 1 activated autophagy and inhibited Tau pathology as revealed by flow cytometric analyses, confocal imaging analysis and western blotting, and this effect was mediated by transcription factor EB (TFEB). These findings suggested that 1 might have potential as a compound for combating Alzheimer's disease.

Alzheimer's disease (AD), the most common type of dementia mainly affecting elderly individuals, is characterized by accumulation of senile plaques and neurofibrillary tangles (NFTs) in the brain which are both toxic to neurons and damage them. Amyloid- β (A β) and hyperphosphorylated microtubule-associated protein tau (MAPT) are the components of senile plaques and NFTs, respectively. The aggregations of A β and MAPT have each been linked to the pathogenesis of AD.¹ Therefore, promoting the clearance of A β and Tau from the

brain constitutes one of the most promising strategies for preventing and treating AD.^{2–7}

The ubiquitin-proteasome system and the autophagy pathway are two major degradation systems for eliminating abnormal proteins in cells.^{8,9} The ubiquitin-proteasome system disposes of most of the short-lived proteins, while the autophagy pathway targets long-lived high-molecular-weight proteins. The main types of autophagy (including macroautophagy, microautophagy, and chaperone-mediated autophagy) are mechanistically different from each other.¹⁰ Macroautophagy, herein referred to as autophagy, is an important machinery for degrading misfolded proteins to maintain homeostasis especially in long-lived cells such as neurons. Autophagy dysfunction has been implicated in the pathogenesis of many neurodegenerative diseases including AD.^{11–18} The requirement of autophagy activation in memory formation further underscores the critical importance of its regulation for brain function.¹⁹ Induction of autophagy may serve as a viable therapeutic strategy for combatting AD.^{15,17,20} Recently, transcription factor EB (TFEB) has been intensively studied for its key role in regulating lysosomal biogenesis and autophagy.^{21–23} TFEB is phosphorylated by the mammalian target of rapamycin complex (mTOR) at Ser142, Ser211 and Ser122 and sequestered in the cytosol when there are sufficient nutrients. TFEB is activated in response to nutrient deprivation and can stimulate translocation to the nucleus to induce lysosomal biogenesis and activate autophagy-related genes.^{23–26} Therefore, finding a TFEB activator may serve as a potential therapeutic strategy for AD.^{27–30}

The genus *Munronia* (Meliaceae) comprises 15 species that are mainly distributed in regions of Asia and Africa; eight of these species and one variant grow in China.³¹ *Munronia henryi* Harms is a low, small semi bush that has been used in Chinese traditional medicine to treat bruises, rheumatic joint pain, coughs, stomachaches, tuberculosis, and sores.³² Previous chemical studies on the *Munronia henryi* Harms plant have revealed the presence of limonoids (munronins A–F and munroniamide), which are major secondary metabolites of

^aState Key Laboratory of Functions and Applications of Medicinal Plants & College of Pharmacy, Guizhou Provincial Engineering Technology Research Center for Chemical Drug R&D, Guizhou Medical University, Guiyang 550014, China

^bKey Laboratory of Animal Models and Human Disease Mechanisms of the Chinese Academy of Sciences & Yunnan Province, KIZ-CUHK Joint Laboratory of Bioresources and Molecular Research in Common Diseases, Kunming Institute of Zoology, Chinese Academy of Sciences, Kunming 650204, China. E-mail: luorongcan@mail.kiz.ac.cn

^cKunming College of Life Science, University of Chinese Academy of Sciences, Kunming, Yunnan 650204, China

^dState Key Laboratory of Phytochemistry and Plant Resources in West China, Kunming Institute of Botany, Chinese Academy of Sciences, Kunming 650201, China. E-mail: haoxj@mail.kib.ac.cn

^eCAS Center for Excellence in Brain Science and Intelligence Technology, Chinese Academy of Sciences, Shanghai 200031, China

†Electronic supplementary information (ESI) available. See DOI: <https://doi.org/10.1039/d2ob01965e>

‡These authors contributed equally to this work.

this species and display potent antifeedant activity.^{33,34} We have found diverse rearranged limonoid derivatives (munronins A–U), which exhibited significant biological activities, such as cytotoxicity³⁵ and antiviral activity against tobacco mosaic virus (TMV),^{35,36} and to serve as potential activators for plant resistance.^{37,38} In this study, we continued our work on the discovery of bioactive molecules from the *Munronia henryi* Harms plant. A new ring-containing A,B-*seco*-limonoid, munronin V (**1**) was isolated from the extracts of the whole plant. Munronin V was found to have a novel 7/7/6 tricyclic framework featuring an unusual ring A,B-*seco*-limonoid (Fig. 1). The absolute configuration of its structure was characterized from spectroscopic data and electronic circular dichroism (ECD) analysis. The A,B-*seco* with two seven-membered lactone rings obtained by performing Baeyer–Villiger oxidation has not yet been found in nature to the best of our knowledge.³⁹ Moreover, the biological activity evaluation results showed **1** having a potential anti-AD effect.

Munronin V (**1**) was obtained as a white amorphous powder. Its molecular formula, C₃₃H₄₂O₁₀, was determined from 1D NMR (Table 1) and positive HRESIMS analysis. HRESIMS data showed an [M + Na]⁺ ion at an *m/z* of 621.2677 (calcd 621.2670), indicating 13 double-bond equivalents. The presence of a carboxyl group was confirmed by the strong absorption bands at 1734 cm⁻¹ in the IR spectrum. The ¹³C NMR spectrum (Table 1) showed 32 resolved carbon resonances corresponding to 8 methyl, 4 methylene, 10 methine (four olefinic and two oxygenated), and 11 quaternary (two olefinic, three oxygenated, and four carbonyl) carbons as distinguished by the HSQC spectrum and DEPT experiments (Fig. S3

Table 1 ¹H (600 Hz) and ¹³C (150 Hz) NMR data of munronin V (**1**) in CDCl₃ (δ in ppm)

No.	δ _H (J in Hz)	δ _C	No.	δ _H (J in Hz)	δ _C
1	5.00, dd (3.2, 11.8)	71.3	16b	2.00, m	
2a	3.06, m	34.5	17	2.84, dd (5.8, 12.2)	42.5
2b	1.66, m		18	1.17, s	15.4
3		169.2	19	1.23, s	14.7
4		85.2	20		122.0
5	2.56, br d (11.8)	47.9	21	7.07, s	140.0
6a	3.22, dd (13.2, 17.8)	35.7	22	5.97, s	111.4
6b	2.70, br d (17.8)		23	7.30, t (6.2)	142.8
7		172.1	28	1.67, s	34.4
8		85.4	29	1.47, s	23.5
9	3.12, br d (15.2)	45.8	30	1.49, s	19.9
10		47.0	1-OAc		169.1
11a	1.97, m	29.3		1.85, s	20.9
11b	1.26, m		1'		168.3
12	5.17, br d (10.8)	76.3	2'		129.5
13		44.8	3'	6.30, q, (5.6)	136.8
14		72.8	4'	1.72, d, (7.2)	14.2
15	3.63, s	56.0	5'	1.81, s	12.2
16a	2.27, m	31.7			

and S2†). In addition, NMR data showed characteristic resonances of the β-substituted furan moiety (δ_H 7.30, 7.07, and 5.97; δ_C 142.8, 140.0, 122.0, and 111.4), and five singlet methyl groups (δ_H 1.67, 1.49, 1.47, 1.23, and 1.17; δ_C 34.4, 23.5, 19.9, 15.4, 14.7). Compound **1** was indicated from these data to contain the limonoid with a tetracyclic core.

Further insights were obtained from an extensive comparison of ¹H and ¹³C NMR data of **1** with those of known limonoids, especially munronin I.³⁵ From a similarity of the chemical shifts of the two compounds in A, D, and E rings, both compounds were suggested to share the same A, D, and E ring systems, which was further confirmed from 2D NMR studies. In addition, ¹H–¹H COSY correlations of H-9/H₂-11, and H-12/H₂-11, and multiple HMBC correlations of H-9/C-8, C-11, H-12/C-9, C-1', C-18, H₃-30/C-8, C-14, and H₃-18/C-12, C-13 and C-14 were observed. These correlations suggested a six-membered ring C with methylene at C-11 and a tigloyloxy unit attached to C-12. The B-ring was assembled into a seven-membered lactone ring according to the key HMBC H-5/C-6, C-7, H₃-19/C-10, and H-9/C-8 and C-10 cross-peaks, along with the ¹H–¹H COSY H-5/H₂-6 cross-peaks. Subsequently, the linkages of C-5 and C-10 were assigned by multiple HMBC correlations of H-5/C-4, C-6, C-7, C-19 and C-29, H₃-19/C-10, and C-1. The HMBC correlation between H₂-6 and C-7 (δ_C 172.1) indicated the connectivity of C-6 and C-3. The terminus of the C-7 ester carbonyl was most likely to form ring B of a seven-membered lactone with the oxygenated C-8, which was severely downfield shifted at δ_C 85.4. Based on these data, the structure of **1** was concluded to be planar.

The relative configuration of compound **1** was established by analyzing ROESY correlations (Fig. S6†). The key ROESY correlations H-5/H-9, H-5/H₃-18, H-5/H₃-28, and H-15/H₃-18 indicated that H-5, H-9, H₃-18 and H₃-28 were cofacial and adopted α-orientations. Similarly, the ROE correlations H-12/

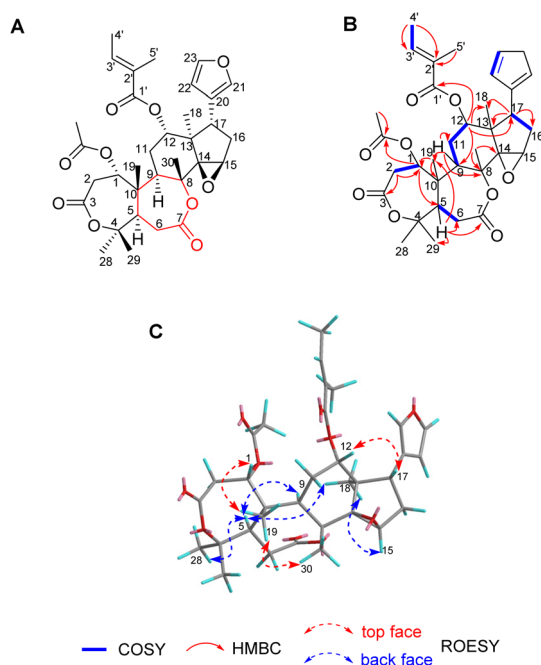


Fig. 1 (A) Structure of munronin V (**1**). (B and C) Key ¹H–¹H COSY, HMBC, and ROESY correlations of **1**.

H-17, H-1/H₃-19, and H₃-19/H₃-30 suggested the cofaciality and β-orientations for these protons. Therefore, these correlations confirmed the relative configuration. To determine the absolute configuration, the ECD spectrum of **1** in MeOH was acquired. The former result was also confirmed by the well-matched ECD data between calculated ECD data of 1*S*, 5*R*, 8*R*, 9*R*, 10*S*, 12*S*, 13*R*, 14*S*, 15*R*, 17*S*, and our isolated **1** (Fig. 2).

A hypothetical biosynthesis pathway to **1** are illustrated in Scheme 1. This pathway may start with azadirone-type limonoid (12α-acetoxy-7-deacetylazadirone),⁴⁰ and have Baeyer-Villiger oxidation playing an important role in the formation of an unprecedented 7/7/6 tricyclic framework. The cleavage sites in lactone rings are located at C-3/C-4 in the A ring, and C-7/C-8 in the B ring. The seven-membered lactone ring (ring B) undergoes C7–C8 bond cleavage to form the new C7–O–C8 ester bond.

In order to determine whether compound **1** would have potential activity for enhancing the autophagy-lysosomal system, we conducted cellular assays using a human microglia

cell line (HM mCherry-GFP-LC3) with stable overexpression of a triple fusion protein (red fluorescent protein (mCherry), green fluorescent protein (GFP), and the autophagosome marker LC3), which can directly reflect the strength of autophagic flux. We treated different samples of the HM mCherry-GFP-LC3 cells with **1** at, respectively, two concentrations (10 μM and 40 μM) for 24 h. Then, the cells were fixed with 4% paraformaldehyde (PFA) before being characterized using flow cytometry analysis. We found that **1** has the ability to activate the autophagic flux (Fig. 3A and B). We also observed, using laser scanning confocal microscopy, an increased number of red puncta and a decreased number of green puncta in the **1**-treated HM mCherry-GFP-LC3 cells (Fig. 3C and D).

To test the potential biological activity of **1** against AD, we conducted cellular assays by using human glioma U251 cells (U251-MAPT P301S cells) stably overexpressing the human MAPT mutant (MAPT-p.P301S). This cell line was used as a cellular AD model. In this assay, we used the solvent of **1** (dimethyl sulfoxide, DMSO) as a negative control and rapamycin (autophagy inducer) as a positive control. There were no obvious morphological changes in various samples of the U251-MAPT P301S cells after they were treated with **1** at concentrations of, respectively, 2.5 μM, 10 μM and 40 μM for 24 h (Fig. 3E). We found that **1** showed activity for activating autophagy and inhibiting Tau pathology, as demonstrated by the increased protein levels of LC3-II/LC3-I and lysosomal hydrolases CTSB (cathepsin B, which plays an important role in lysosome dynamics and autophagy^{41,42}), and decreased protein levels of Tau P301S and SQSTM1 (Fig. 3F). Moreover, we found that the TFEB level was significantly increased, whereas the phospho-TFEB (Ser122) (p-TFEB (Ser 122)) level was significantly decreased (Fig. 3F), suggesting that TFEB was activated by **1**.

To further check the activity of **1** towards activating TFEB, we carried out tests with HM TFEB-GFP cells (which stably

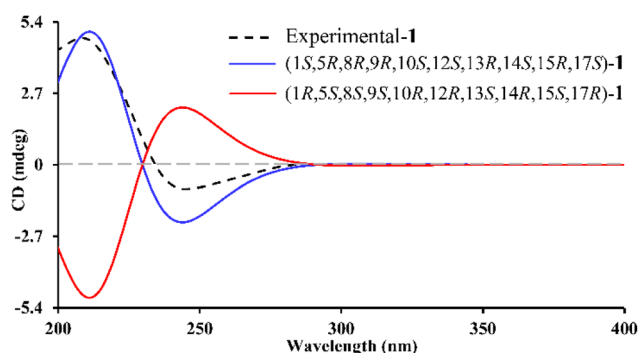
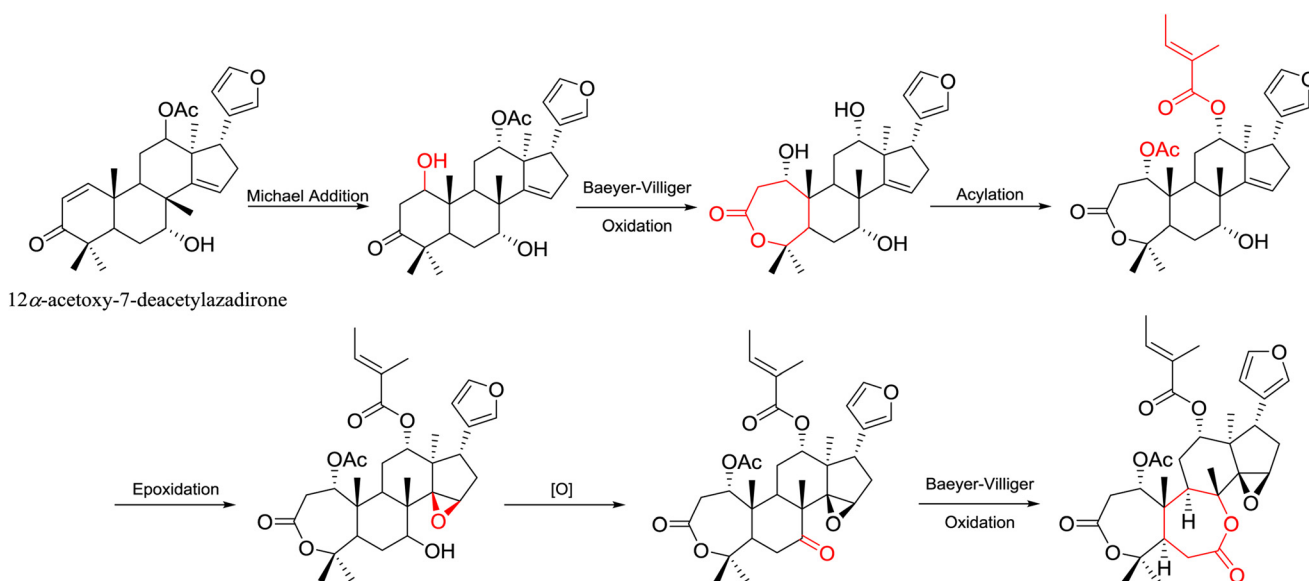


Fig. 2 Experimental and computational ECD spectra of compound **1**.



Scheme 1 Hypothetical biosynthetic pathway to compound **1**.

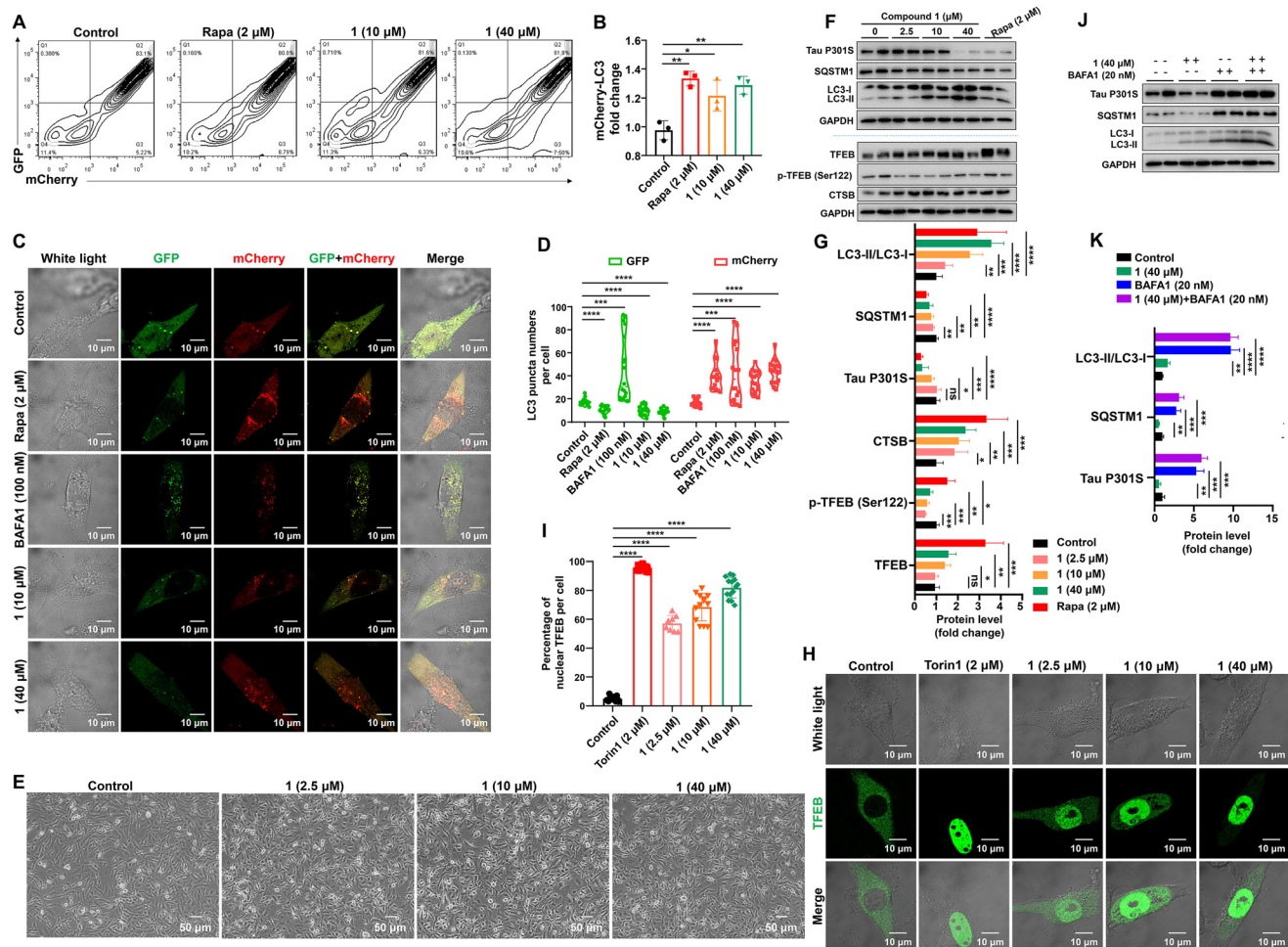


Fig. 3 Results of biological activity assays. (A) Flow cytometry of samples of HM mCherry-GFP-LC3 cells treated with **1** and rapamycin (Rapa), respectively. The percentage of 10 000 cells that expressed GFP and/or mCherry protein was counted. Rapamycin (Rapa) was used as a positive control and DMSO was used as a negative control (Control). (B) Quantification of the cells with only mCherry puncta in (A), with Rapa used as a positive control. (C) Representative images of samples of HM mCherry-GFP-LC3 cells treated with compound **1** at indicated concentrations, Rapa, bafilomycin A1 (BAFA1), and DMSO (Control), respectively. Scale bars, 10 μ m. (D) Quantification of the LC3 puncta in (C) based on 3 independent experiments. (E) Morphologies of samples of U251-MAPT P301S cells treated for 24 h with indicated concentrations of **1** (2.5 μ M, 10 μ M and 40 μ M, respectively) as well as of a sample treated for 24 h with DMSO as a negative control (Control). (F and G) Western blotting results showing the protein levels of Tau P301S, LC3-II/LC3-I, SQSTM1, TFEB, p-TFEB (Ser122), CTSB and GAPDH in samples of U251-MAPT P301S cells treated with or without indicated concentrations of compound **1**. Rapa was used as a positive control. Shown data include (F) representative western blotting results and (G) quantification of protein levels based on 3 independent experiments. (H) Representative images of samples of HM TFEB-GFP cells treated with indicated concentrations of **1**. Torin1 was used as a positive control and DMSO as a negative control (Control). (I) Quantifications of the proportion of nuclear TFEB in (H). (J and K) Western blotting results showing the protein levels of Tau P301S, LC3-II/LC3-I, SQSTM1, and GAPDH in the U251-MAPT P301S cells treated with or without compound **1** and/or BAFA1. GAPDH was used as the loading control for western blotting. Data are presented as means \pm SD. ns, not significant; **** P < 0.0001; *** P < 0.001; ** P < 0.01; * P < 0.05; one-way ANOVA with Dunnett's *post-hoc* test.

overexpress TFEB-GFP). In this assay, we used Torin1 (2 μ M) as a positive control.^{22,24} We treated the HM TFEB-GFP cells with **1** or Torin1 for 6 h, and then fixed the cells with 4% PFA, followed by subjecting them to confocal analysis. We found that **1** promoted the translocation of TFEB from the cytoplasm into the nucleus in a dose-dependent manner (Fig. 3H and I). To further determine the vital role of autophagy in reducing Tau P301S levels, as a control we used bafilomycin A1 (BAFA1), which inhibits the fusion of autophagosomes with lysosomes, leading to accumulation of LC3II and blocking of the autophagy process.^{43,44} Treatment of U251-MAPT P301S cells with

BAFA1 had no significant effect on Tau P301S protein levels, but led to increased LC3II/LC3I and SQSTM1 levels, consistent with the effect of BAFA1. However, treatment of the cells with both **1** and BAFA1 reversed the decreased levels of Tau P301S compared to treatment with **1** alone (Fig. 3J and K). These results suggested that **1** increased Tau P301S clearance through the autophagy-lysosomal pathway.

Based on the above results, we speculated that potential intermolecular interactions can form between **1** and TFEB. A molecular docking analysis was carried out to confirm this speculation. As shown in Fig. S10,[†] compound **1** could

bind to the active site of TFEB in a proposed pose illustrated with a predicted binding energy of $-6.47 \text{ kcal mol}^{-1}$. **1** might form hydrogen bonds with TFEB at GLN10 and ARG13, and hydrophobic interactions at MET9 and PRO51. All these bonds and interactions would help stabilize the binding of compound **1** to TFEB and affect the activity of TFEB.

In conclusion, munronin V (**1**) is, to the best of our knowledge, the first example of the unprecedented 7/7/6 tricyclic framework featuring an unusual ring, A,B-*seco*-limonoid, from *M. henryi*. The potential bioactivity of **1** against AD, involving its promoting the clearance of Tau *via* TFEB-mediated autophagy, was proved in cellular models based on several lines of evidence: (1) **1** promoted autophagy in HM mCherry-GFP-LC3 cells as indicated by flow cytometry and confocal analysis; (2) Tau P301S production was significantly decreased after U251-MAPT P301S cells were treated with **1**; (3) **1** activated the autophagy-lysosome system as indicated by its inclusion leading to increased levels of CTSB, TFEB, LC3-II/LC3-I, and decreased levels of SQSTM1, p-TFEB (Ser122); and (4) **1** induced autophagy through the activation of TFEB and decreased Tau P301S level, which was abrogated by BAFA1. Taken together, **1** might be an effective compound for treating AD, and it would be rewarding to examine cognitive function changes upon treating AD animal models with **1**.

Conflicts of interest

There are no conflicts to declare.

Acknowledgements

The work was supported financially by the National Natural Science Foundation of China (No. 31160374 to Y.Y., 32170988 and 31900737 to R.L.), Guizhou Provincial Science and Technology projects (No. ZK [2022]393 to Y.Y.), the Original Innovation Project “from 0 to 1” of the Basic Frontier Scientific Research Program, CAS (ZDBS-LY-SM031 to R.L.), the Scientific and Technological Foundation of Guizhou Health Committee (gzwkj2022-222 to Y.Y.), the Cultivation Project of the National Natural Science Foundation from Guizhou Medical University (19NSP083 to Y.Y.), the Basic Research Program of Yunnan Province (202201AW070010 and 202001AT070107 to R.L., and 202003AD150009), the Youth Innovation Promotion Association of CAS (2021000011 to R.L.), the Strategic Priority Re-search Program (B) of CAS (XDB02020003 to Y.G.Y.), the CAS “Light of West China” Program (2020000023 to R.L.), the Young Scientific and Technological Talents Promotion Project of Yunnan Association for Science and Technology (2022000043 to R.L.), and the Open Project from Key Laboratory of Animal Models and Human Disease Mechanisms of the Chinese Academy of Sciences & Yunnan Province (AMHD-2021-4 and AMHD-2022-4).

References

- D. S. Knopman, H. Amieva, R. C. Petersen, G. Chételet, D. M. Holtzman, B. T. Hyman, R. A. Nixon and D. T. Jones, *Nat. Rev. Dis. Primers*, 2021, **7**, 33.
- X. L. Bu, Y. Xiang, W. S. Jin, J. Wang, L. L. Shen, Z. L. Huang, K. Zhang, Y. H. Liu, F. Zeng, J. H. Liu, H. L. Sun, Z. Q. Zhuang, S. H. Chen, X. Q. Yao, B. Giunta, Y. C. Shan, J. Tan, X. W. Chen, Z. F. Dong, H. D. Zhou, X. F. Zhou, W. Song and Y. J. Wang, *Mol. Psychiatry*, 2017, **23**, 1948–1956.
- E. E. Congdon and E. M. Sigurdsson, *Nat. Rev. Neurol.*, 2018, **14**, 399–415.
- W.-S. Jin, L.-L. Shen, X.-L. Bu, W.-W. Zhang, S.-H. Chen, Z.-L. Huang, J.-X. Xiong, C.-Y. Gao, Z. Dong, Y.-N. He, Z.-A. Hu, H.-D. Zhou, W. Song, X.-F. Zhou, Y.-Z. Wang and Y.-J. Wang, *Acta Neuropathol.*, 2017, **134**, 207–220.
- D. J. Selkoe and J. Hardy, *EMBO Mol. Med.*, 2016, **8**, 595–608.
- L. Bakota and R. Brandt, *Drugs*, 2016, **76**, 301–313.
- J. T. Pedersen and E. M. Sigurdsson, *Trends Mol. Med.*, 2015, **21**, 394–402.
- C. Pohl and I. Dikic, *Science*, 2019, **366**, 818–822.
- J. L. Sun-Wang, A. Yarritu-Gallego, S. Ivanova and A. Zorzano, *Trends Endocrinol. Metab.*, 2021, **32**, 594–608.
- D. J. Klionsky, A. K. Abdel-Aziz, S. Abdelfatah, M. Abdellatif, A. Abdoli, S. Abel, H. Abeliovich, M. H. Abildgaard, Y. P. Abudu, A. Acevedo-Arozena, I. E. Adamopoulos, *et al.*, *Autophagy*, 2021, **17**, 1–382.
- T. Hara, K. Nakamura, M. Matsui, A. Yamamoto, Y. Nakahara, R. Suzuki-Migishima, M. Yokoyama, K. Mishima, I. Saito, H. Okano and N. Mizushima, *Nature*, 2006, **441**, 885–889.
- H. Harris and D. C. Rubinsztein, *Nat. Rev. Neurol.*, 2011, **8**, 108–117.
- M. Komatsu, S. Waguri, T. Chiba, S. Murata, J.-i. Iwata, I. Tanida, T. Ueno, M. Koike, Y. Uchiyama, E. Kominami and K. Tanaka, *Nature*, 2006, **441**, 880–884.
- R. Luo, Y. Fan, J. Yang, M. Ye, D.-F. Zhang, K. Guo, X. Li, R. Bi, M. Xu, L.-X. Yang, Y. Li, X. Ran, H.-Y. Jiang, C. Zhang, L. Tan, N. Sheng and Y.-G. Yao, *Signal Transduction Targeted Ther.*, 2021, **6**, 325.
- R. Luo, L.-Y. Su, G. Li, J. Yang, Q. Liu, L.-X. Yang, D.-F. Zhang, H. Zhou, M. Xu, Y. Fan, J. Li and Y.-G. Yao, *Autophagy*, 2020, **16**, 52–69.
- F. M. Menzies, A. Fleming and D. C. Rubinsztein, *Nat. Rev. Neurosci.*, 2015, **16**, 345–357.
- V. Schaeffer and M. Goedert, *Autophagy*, 2014, **8**, 1686–1687.
- L. Y. Su, H. Li, L. Lv, Y. M. Feng, G. D. Li, R. Luo, H. J. Zhou, X. G. Lei, L. Ma, J. L. Li, L. Xu, X. T. Hu and Y. G. Yao, *Autophagy*, 2015, **11**, 1745–1759.
- M. Glatigny, S. Moriceau, M. Rivagorda, M. Ramos-Brossier, A. C. Nascimbeni, F. Lante, M. R. Shanley, N. Boudarene, A. Rousseaud, A. K. Friedman, C. Settembre, N. Kuperwasser, G. Friedlander, A. Buisson, E. Morel, P. Codogno and F. Oury, *Curr. Biol.*, 2019, **29**, 435–448.

- 20 A. Di Meco, J.-G. Li, B. E. Blass, M. Abou-Gharbia, E. Lauretti and D. Praticò, *Biol. Psychiatry*, 2017, **81**, 92–100.
- 21 H. Martini-Stoica, Y. Xu, A. Ballabio and H. Zheng, *Trends Neurosci.*, 2016, **39**, 221–234.
- 22 Y. Li, M. Xu, X. Ding, C. Yan, Z. Song, L. Chen, X. Huang, X. Wang, Y. Jian, G. Tang, C. Tang, Y. Di, S. Mu, X. Liu, K. Liu, T. Li, Y. Wang, L. Miao, W. Guo, X. Hao and C. Yang, *Nat. Cell Biol.*, 2016, **18**, 1065–1077.
- 23 C. Settembre, C. Di Malta, V. A. Polito, M. Garcia Arencibia, F. Vetrini, S. Erdin, S. U. Erdin, T. Huynh, D. Medina, P. Colella, M. Sardiello, D. C. Rubinsztein and A. Ballabio, *Science*, 2011, **332**, 1429–1433.
- 24 S. Vega-Rubin-de-Celis, S. Pena-Llopis, M. Konda and J. Brugarolas, *Autophagy*, 2017, **13**, 464–472.
- 25 R. David, *Nat. Rev. Mol. Cell Biol.*, 2011, **12**, 404.
- 26 A. M. Cuervo, *Science*, 2011, **332**, 1392–1393.
- 27 C. Yang, C. Su, A. Iyaswamy, S. K. Krishnamoorthi, Z. Zhu, S. Yang, B. C. Tong, J. Liu, S. G. Sreenivasmurthy, X. Guan, Y. Kan, A. J. Wu, A. S. Huang, J. Tan, K. Cheung, J. Song and M. Li, *Acta Pharm. Sin. B*, 2022, **12**, 1707–1722.
- 28 X. Zheng, W. Lin, Y. Jiang, K. Lu, W. Wei, Q. Huo, S. Cui, X. Yang, M. Li, N. Xu, C. Tang and J. X. Song, *Autophagy*, 2021, **17**, 3833–3847.
- 29 Y. Xu, S. Du, J. A. Marsh, K. Horie, C. Sato, A. Ballabio, C. M. Karch, D. M. Holtzman and H. Zheng, *Mol. Psychiatry*, 2021, **26**, 5925–5939.
- 30 J. X. Song, S. Malampati, Y. Zeng, S. S. K. Durairajan, C. B. Yang, B. C. Tong, A. Iyaswamy, W. B. Shang, S. G. Sreenivasmurthy, Z. Zhu, K. H. Cheung, J. H. Lu, C. Tang, N. Xu and M. Li, *Aging Cell*, 2020, **19**, e13069.
- 31 H.-P. Zhang, G.-H. Bao, H.-B. Wang and G.-W. Qin, *Nat. Prod. Res.*, 2004, **18**, 415–419.
- 32 S.-H. Qi, D.-G. Wu, Y.-B. Ma and X.-D. Luo, *J. Asian Nat. Prod. Res.*, 2003, **5**, 215–221.
- 33 S.-H. Qi, D.-G. Wu, L. Chen, Y.-B. Ma and X.-D. Luo, *J. Agric. Food Chem.*, 2003, **51**, 6949–6952.
- 34 S.-H. Qi, L. Chen, D.-G. Wu, Y.-B. Ma and X.-D. Luo, *Tetrahedron*, 2003, **59**, 4193–4199.
- 35 Y. Yan, J.-X. Zhang, T. Huang, X.-Y. Mao, W. Gu, H.-P. He, Y.-T. Di, S.-L. Li, D.-Z. Chen, Y. Zhang and X.-J. Hao, *J. Nat. Prod.*, 2015, **78**, 811–821.
- 36 Y. Yan, C.-M. Yuan, Y.-T. Di, T. Huang, Y.-M. Fan, Y. Ma, J.-X. Zhang and X.-J. Hao, *Fitoterapia*, 2015, **107**, 29–35.
- 37 Y. Yan, L. Tang, J. Hu, J. Wang, T. A. Adelakun, D. Yang, Y. Di, Y. Zhang and X. Hao, *Pestic. Biochem. Physiol.*, 2018, **146**, 13–18.
- 38 Y. Yan, D. Wang, X. Zhang, M. Peng, X. Yan, Y. Guo, M. Jia, J. Zhou, L. Tang and X. Hao, *Pestic. Biochem. Physiol.*, 2022, **184**, 105108.
- 39 Q.-G. Tan and X.-D. Luo, *Chem. Rev.*, 2011, **111**, 7437–7522.
- 40 B. N. Irungu, N. Adipo, J. A. Orwa, F. Kimani, M. Heydenreich, J. O. Midiwo, P. M. Björemark, M. Håkansson, A. Yenesew and M. Erdélyi, *J. Ethnopharmacol.*, 2015, **174**, 419–425.
- 41 S. M. Man and T. D. Kanneganti, *Autophagy*, 2016, **12**, 2504–2505.
- 42 P. Rusmini, K. Cortese, V. Crippa, R. Cristofani, M. E. Cicardi, V. Ferrari, G. Vezzoli, B. Tedesco, M. Meroni, E. Messi, M. Piccolella, M. Galbiati, M. Garre, E. Morelli, T. Vaccari and A. Poletti, *Autophagy*, 2019, **15**, 631–651.
- 43 C. Mauvezin and T. P. Neufeld, *Autophagy*, 2015, **11**, 1437–1438.
- 44 D. C. Rubinsztein, A. M. Cuervo, B. Ravikumar, S. Sarkar, V. Korolchuk, S. Kaushik and D. J. Klionsky, *Autophagy*, 2009, **5**, 585–589.

Supplementary Information

Munronin V with 7/7/6 Tricarbocyclic Framework from *Munronia henryi* Harms Inhibits Tau Pathology via Activating Autophagy

Ying Yan ^{a,‡}, Xiaoqian Ran ^{b,c,‡}, Dan Wang ^a, Xiong Zhang ^a, Mingyou Peng ^a, Xiaoyan Yan ^a, Lei Tang ^a, Hong Liang ^d, Xujie Qin ^d, Ying-Tong Di ^d, Rongcan Luo ^{b,c,*}, Xiao-Jiang Hao ^{d,*}, Yong-Gang Yao ^{b,c,e}

^a State Key Laboratory of Functions and Applications of Medicinal Plants & College of pharmacy, Guizhou Provincial Engineering Technology Research Center for Chemical Drug R&D, Guizhou Medical University, Guiyang 550014, China

^b Key Laboratory of Animal Models and Human Disease Mechanisms of the Chinese Academy of Sciences & Yunnan Province, KIZ-CUHK Joint Laboratory of Bioresources and Molecular Research in Common Diseases, Kunming Institute of Zoology, Chinese Academy of Sciences, Kunming 650204, China

^c Kunming College of Life Science, University of Chinese Academy of Sciences, Kunming, Yunnan 650204, China

^d State Key Laboratory of Phytochemistry and Plant Resources in West China, Kunming Institute of Botany, Chinese Academy of Sciences, Kunming 650201, China

^e CAS Center for Excellence in Brain Science and Intelligence Technology, Chinese Academy of Sciences, Shanghai 200031, China

‡These authors contributed equally to this work.

These authors contributed equally to this work

* Corresponding authors

Rong-Can Luo – *Key Laboratory of Animal Models and Human Disease Mechanisms of the Chinese Academy of Sciences & Yunnan Province, Kunming Institute of Zoology, Chinese Academy of Sciences, Kunming 650223, China; orcid.org/0000-0003-4472-7079 Email: luorongcan@mail.kiz.ac.cn*

Xiao-Jiang Hao – *State Key Laboratory of Phytochemistry and Plant Resources in West China, Kunming Institute of Botany, Chinese Academy of Sciences, Kunming 650201, China; orcid.org/0000-0001-9496-2152 Email: haoxj@mail.kib.ac.cn*

Materials and methods	3
General experimental procedures	3
Plant material	3
Extraction and Isolation	3
Molecular docking method	4
Construction of U251 cells with stable expression of the mutant MAPT (MAPTmut) gene.....	4
Construction of HM cells with stable expression of TFEB gene	5
Flow cytometry analysis	5
Confocal laser scanning assay	6
Western blotting.....	6
Statistics and reproducibility	7
Original spectroscopic data	8
Figure S1. ¹ H NMR (600 MHz) spectrum of munronin V (1) in CDCl ₃	8
Figure S2. ¹³ C NMR (150 MHz) spectrum of munronin V (1) in CDCl ₃	9
Figure S3. HSQC (600 MHz) spectrum of munronin V (1) in CDCl ₃	10
Figure S4. HMBC (600 MHz) spectrum of munronin V (1) in CDCl ₃	11
Figure S5. ¹ H- ¹ H COSY (600 MHz) spectrum of munronin V (1) in CDCl ₃	12
Figure S6. ROESY (600 MHz) spectrum of munronin V (1) in CDCl ₃	13
Figure S7. HRESIMS spectrum of munronin V (1).	14
Figure S8. IR spectrum of munronin V (1).....	15
Figure S9. UV spectrum of munronin V (1).....	16
Figure S10. The molecular docking mode of munronin V (1) and with TFEB.....	17
Figure S11. The raw images of the western blot in in Figure 3.....	18
Reference	18

Materials and methods

General experimental procedures

Optical rotation measurements were conducted with a Jasco P-1020 automatic polarimeter. CD spectra were determined on the Applied Photophysics circular dichroism spectrometer (Applied Photophysics, Leatherhead, Surrey, UK). IR spectra were recorded on a NICOLET iS107 Mid-infrared spectrometer. High-resolution MS data were performed on an Agilent 1290 UPLC/6540 Q-TOF mass spectrometer in positive mode. ^1H , ^{13}C , ^1H - ^1H COSY, HSQC, HMBC and ROESY spectra were collected on Bruker DRX-600 instruments (Bruker, Bremerhaven, Germany). Semi-preparative HPLC separations were performed on an Agilent 1260 liquid chromatograph (Agilent Technologies, USA) with a Waters X-bridge column (5 μm , 10 \times 250 mm). Analytical TLC systems were carried out on silica gel 60 F254 plates (Qingdao Marine Chemical Inc., Qingdao, China). Column chromatography (CC) was performed by using silica gel (200-300 mesh and 60-80 mesh, Qingdao Marine Chemical, Inc., Qingdao, China) and Lichroprep RP-18 gel (40 – 63 μm ; Merck, Darmstadt, Germany). Sephadex LH-20 (40 – 70 μm , Amersham Pharmacia Biotech AB, Uppsala, Sweden). Spots were visualized by heating silica gel plates sprayed with 5% H_2SO_4 in ethanol.

Plant material

The whole plant of *Munronia henryi* was collected in August 2017 from Xingyi, Guizhou Province, China, and was identified by Prof. De-Yuan Chen of Guiyang College of Traditional Chinese Medicine. A voucher specimen (DHL 20170801) was deposited at the Laboratory of Guizhou Medical University.

Extraction and isolation

The air-dried and powdered twigs of *M. henryi* (9.0 kg) were refluxed with 95% ethanol (3 \times 35 L) three times (3 \times 3 h). To obtain the residue (602 g), the combined extract was concentrated under reduced pressure by a rotary evaporator. The extract

was suspended in water and then partitioned with ethyl acetate (4 × 5 L). The ethyl acetate portion (193 g) was applied to a silica gel column using PE–EtOAc (50:1–1:1, v/v) and CH₂Cl₂–CH₃OH (15:1–1:1, v/v) to obtain seven fractions (Fr. 1–Fr. 7). Fr. 6 (21.4 g) was applied to an MCI gel column and eluted with a gradient of CH₃OH/H₂O (30:70 to 95:5) to yield six fractions (Fr. 6A–Fr. 6F). Fr. 6D (27.5 g) was separated by reversed-phase column (CH₃OH–H₂O, 4:6–9:1) to get five fractions (Fr. 6D1–Fr. 6D4). Fr. 6D3 (0.6 g) was purified by Sephadex LH-20 eluting with MeOH to yield three fractions. Fr. 6D3b was further separated by semi-preparative HPLC with an X-bridge column and eluted with CH₃CN /H₂O (2.5 mL/min, CH₃OH: H₂O = 60:40, v/v) to yield compounds **1** (8 mg, $t_R = 28$ min).

Molecular docking method

The full-length human transcription factor EB (TFEB) structural model was established using the ab initio and hierarchical approach based on I-TASSER (<https://zhanglab.ccmb.med.umich.edu/I-TASSER/>)^{1, 2}. The best confirmation was refined with energy minimization and molecular docking was performed by Autodock Vina with center box: $x = 82.509$, $y = 68.741$, $z = 70.767$ and the dimensions: $30 \times 30 \times 30$ Å for TFEB. The docking results were analyzed and shown with Discovery Studio Visualizer (BIOVIA, San Diego, USA) and PyMOL software (Schrodinger, LLC: NY, USA)

Construction of the U251 cells with stable overexpression of the mutant MAPT (MAPTmut) and HM cells with stable overexpression of the *TFEB* gene

The U251 cells, human microglia (HM) cells, HEK293T cells were introduced from the Kunming Cell Bank, Kunming Institute of Zoology, Chinese Academy of Sciences. The U251 cells were maintained in Roswell Park Memorial Institute 1640 supplemented with 10% fetal bovine serum (FBS) (Gibco, USA, 10099-141). The

HEK293T cells and HM cells were maintained in Dulbecco's Modified Eagle Medium (DMEM) supplemented with 10% FBS (Gibco, USA, 10099-141) at 37°C incubator with 5% CO₂ and 95% humidity.

The coding region of the *MAPT* gene with flag tag was cloned into PLVX vector (PLVX-MAPT) of the Lenti-X Tet-On Advanced Inducible Expression System (Clontech). Mutant MAPT P301S was introduced into PLVX-MAPT vector by using site-directed mutagenesis PCR method. The U251 cells with stable overexpression of mutant MAPT P301S were established according to the instruction of Lenti-X Tet-On Advanced Inducible Expression System (Clontech) and following our previously reported method³. In brief, the response lentivirus system was composed of mutant PLVX-MAPT construct, packaging plasmid psPAX2 (Addgene, England, 12260), and envelope plasmid PMD2.G (Addgene, England, 12259), while the regulator lentivirus system was composed of PLVX-Tet-On-Advanced vector, psPAX2 and PMD2.G. The lentivirus supernatant was produced from the HEK293T cells and was used to infect U251 cells with a ratio of 4:1 for the response lentivirus and the regulator lentivirus. Infected U251 cells were selected in growth medium with 1µg/mL puromycin.

The coding region of the *TFEB* gene with flag tag was cloned into PLVX vector (PLVX-TFEB). The response lentivirus system and the regulator lentivirus system were same to the above one for making MAPT P301 overexpression, except for replacing mutant PLVX-MAPT construct with the PLVX-TFEB construct. HM cells were infected with the lentivirus systems and were selected in growth medium with and 1µg/mL puromycin.

Flow cytometry analysis

The flow cytometry analysis was performed as described in our previous study⁴. In brief, HM mCherry-GFP-LC3 cells with stable overexpression of a triple fusion protein (red fluorescent protein (mCherry), green fluorescent protein (GFP) and the autophagosome marker LC3), was constructed as a cell line for quantifying the strength of autophagic flux. The bioactivity of compound **1** was evaluated in the HM

mCherry-GFP-LC3 cells. Briefly, HM mCherry-GFP-LC3 cells were cultured in DMEM supplemented with 10% fetal bovine serum (Gibco-BRL, 10099-141) at 37°C incubator with 5% CO₂ and 95% humidity. The HM mCherry-GFP-LC3 cells (2x10⁵/well) were cultured in 12-well plates overnight, then were treated with different concentrations of the compound (10 μM and 40 μM; compound was directly added into the culture medium). After 24-hour treatment of compound **1**, cells were fixed by 4% PFA (paraformaldehyde), followed by a flow cytometry test to check whether the autophagic flux was enhanced through analyzing the ratio of cells with red fluorescence which means the autophagic flux goes well as the acid-sensitive GFP was quenched by autolysosome⁵. Data were analyzed using FlowJo software (FLOWJO, LLC). This experiment was repeated at least 3 times, with 3 biological replicates for each treatment.

Confocal laser scanning assay

The HM mCherry-GFP-LC3 cells were cultured in glass-bottom cell dish (NEST, 801001). After the treatment of compound **1**, Rapamycin and Bafilomycin A1 (BAFA1) for 24 h, cells were fixed by 4% PFA and then were individually pictured under an Olympus FluoView™ 1000 confocal microscope (Olympus, Japan). The HM TFEB-GFP cells were handled the same way, with the exception of a shorter treatment with compound **1** and Torin1 for 6 h. Images were analyzed with FV10-ASW 2.1 Viewer (OlympusMicro, Japan).

Western blotting

The U251-MAPT P301S cells were cultured in 6-well plates. Western blotting for target proteins was performed using the common approach as described in our previous studies⁶⁻⁸. Briefly, a protein lysis buffer (Beyotime Institute of Biotechnology, P0013) was used for making cell lysates. After the protein concentration in cell lysate was determined by using the BCA protein assay kit (Beyotime Institute of Biotechnology, P0012), about 20 μg total proteins were separated by 12% sodium dodecyl sulfate polyacrylamide gel electrophoresis and were transferred to polyvinylidene difluoride membrane (Bio-Rad, L1620177 Rev D).

The membrane was blocked in 5% (w:v) skim milk at room temperature for 2 hours. The membrane was incubated with primary antibody against Tau (1:1000, cell signaling technology, 46687S), TFEB (1:1000; cell signaling technology, 4240S), p-TFEB Ser122 (1:1000; cell signaling technology, 86843S), CTSB (1:1000; Affinity, AF5189), SQSTM1 (1:1000, Elabscience, E-AB-62289), LC3 (1:1000, Proteintech, 14600-1-AP), GAPDH (1:20000, Affinity, AF7021), at 4°C overnight, respectively. The membrane was washed 3 times with TBST (Tris buffered saline [Servicebio, G0001] with 0.1% Tween 20 [Sangon Biotech (Shanghai) Co.,Ltd, HB09BA0007]) for 5 min each time, and incubated with either peroxidase-conjugated anti-mouse (KPL; 474-1806; 1:10000) or anti-rabbit IgG (KPL; 474-1516; 1:10000; KPL) at room temperature for 1 hour. The epitope was visualized using ECL Western Blot Detection Kit (Millipore, WBKLS0500). Western blot of GAPDH was used as an inner control for measuring the target protein level. The densitometry of target protein was evaluated by ImageJ software (National Institutes of Health, Bethesda, Maryland, USA).

Statistics and reproducibility

Data analyses were carried out by using GraphPad Prism 8 (GraphPad Software, Inc., La Jolla, CA, USA). The one-way ANOVA (analysis of variance) was performed using the Dunnett's *post hoc* test for comparison between the treated group and control group, and the values were expressed as mean \pm standard deviation (SD). The difference was considered to be statistically significant if a *P* value < 0.05 . *, *P* < 0.05 ; **, *P* < 0.01 ; ***, *P* < 0.001 ; ****, *P* < 0.0001 .

Original spectroscopic data

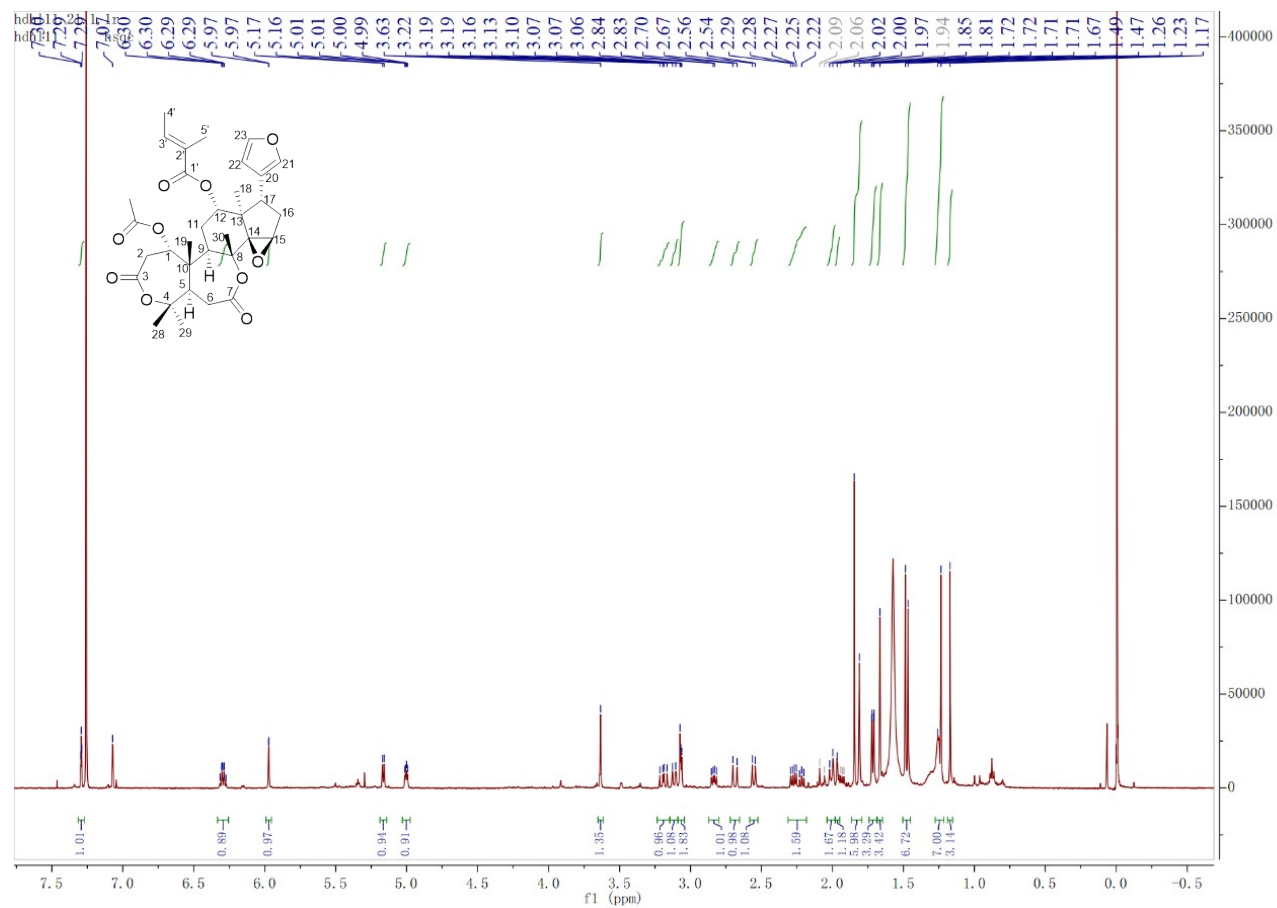


Figure S1. ¹H NMR (600 MHz) spectrum of munronin V (1) in CDCl₃.

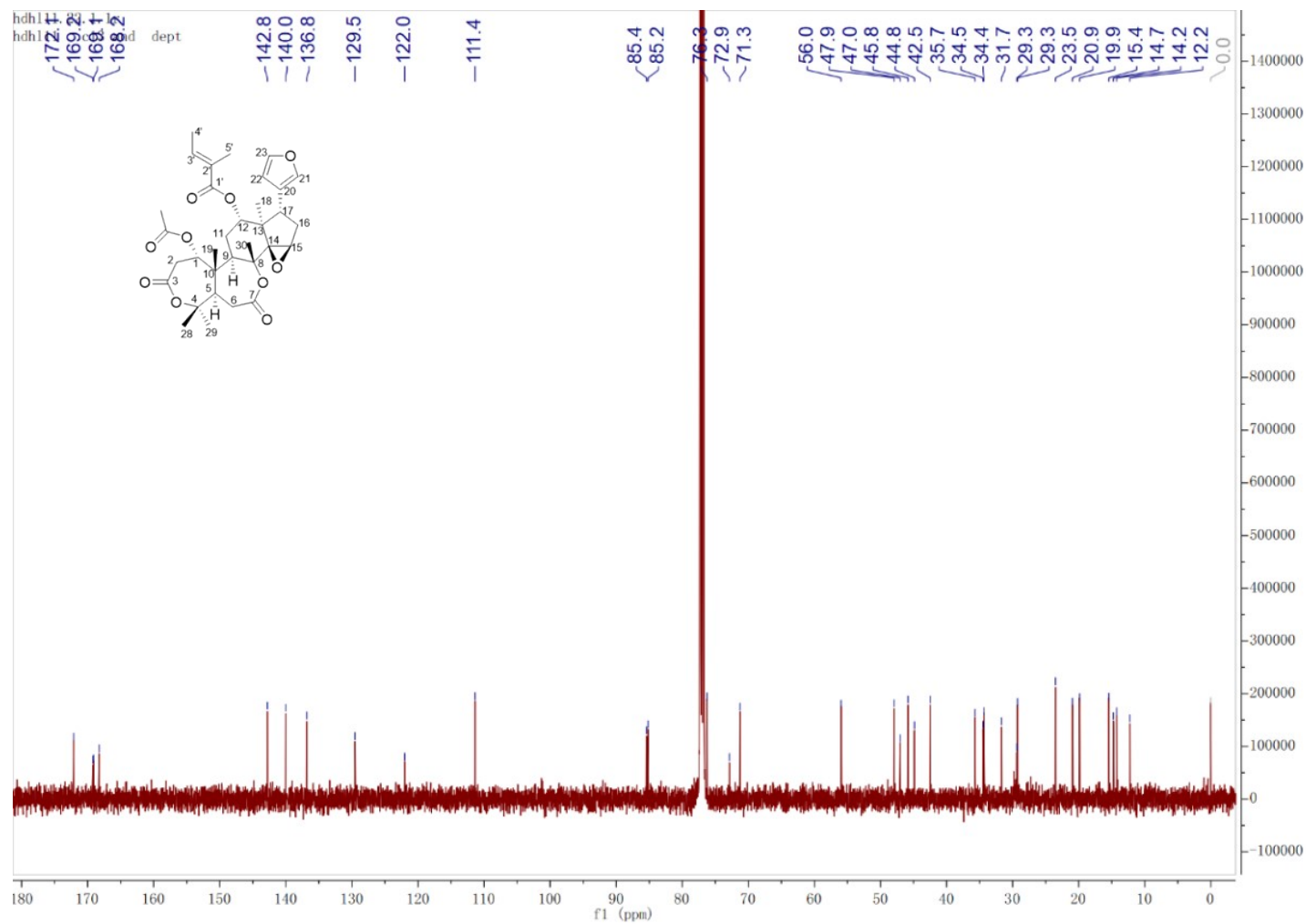


Figure S2. ^{13}C NMR (150 MHz) spectrum of munronin V (1) in CDCl_3 .

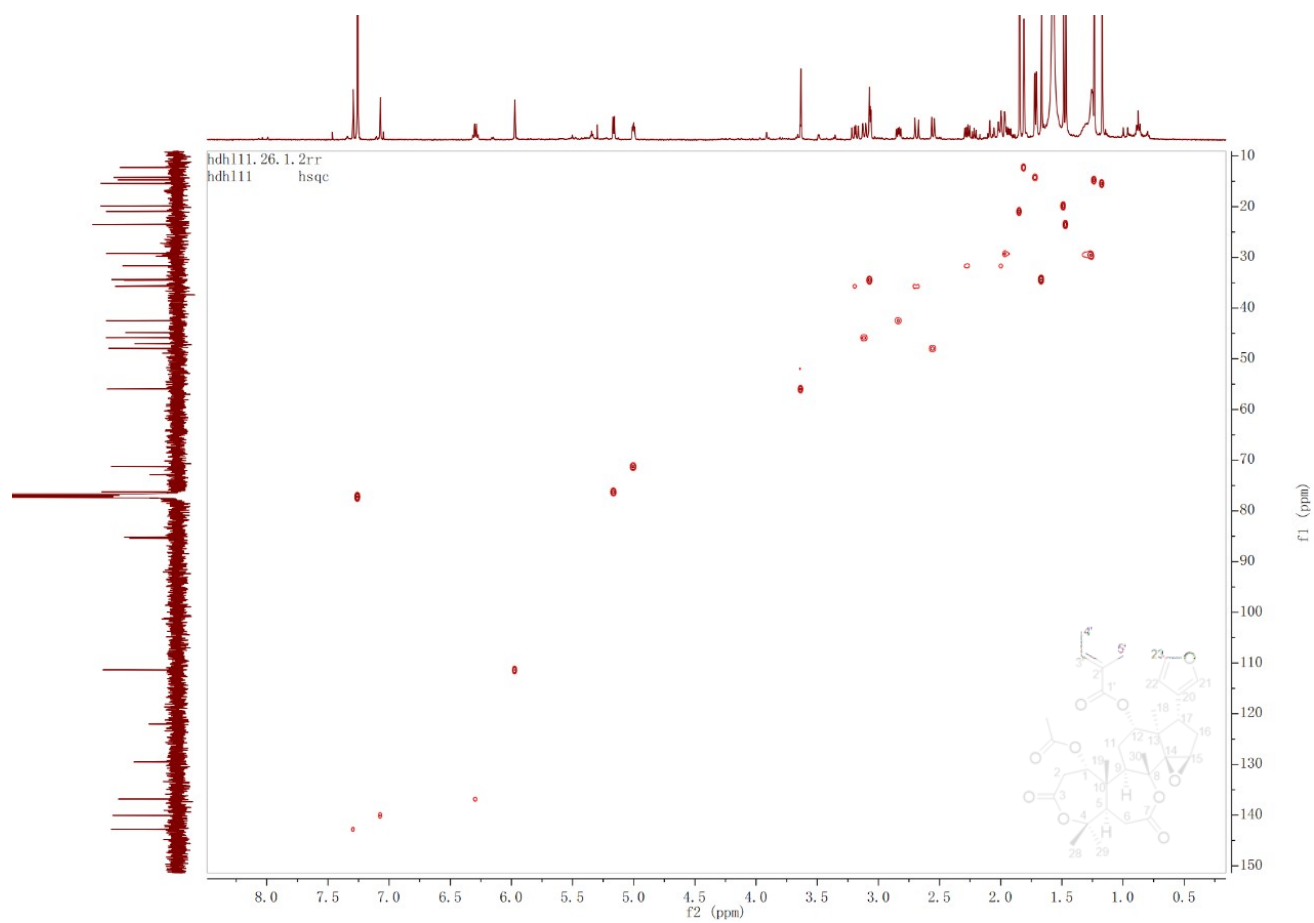


Figure S3. HSQC (600 MHz) spectrum of munronin V (1) in CDCl₃.

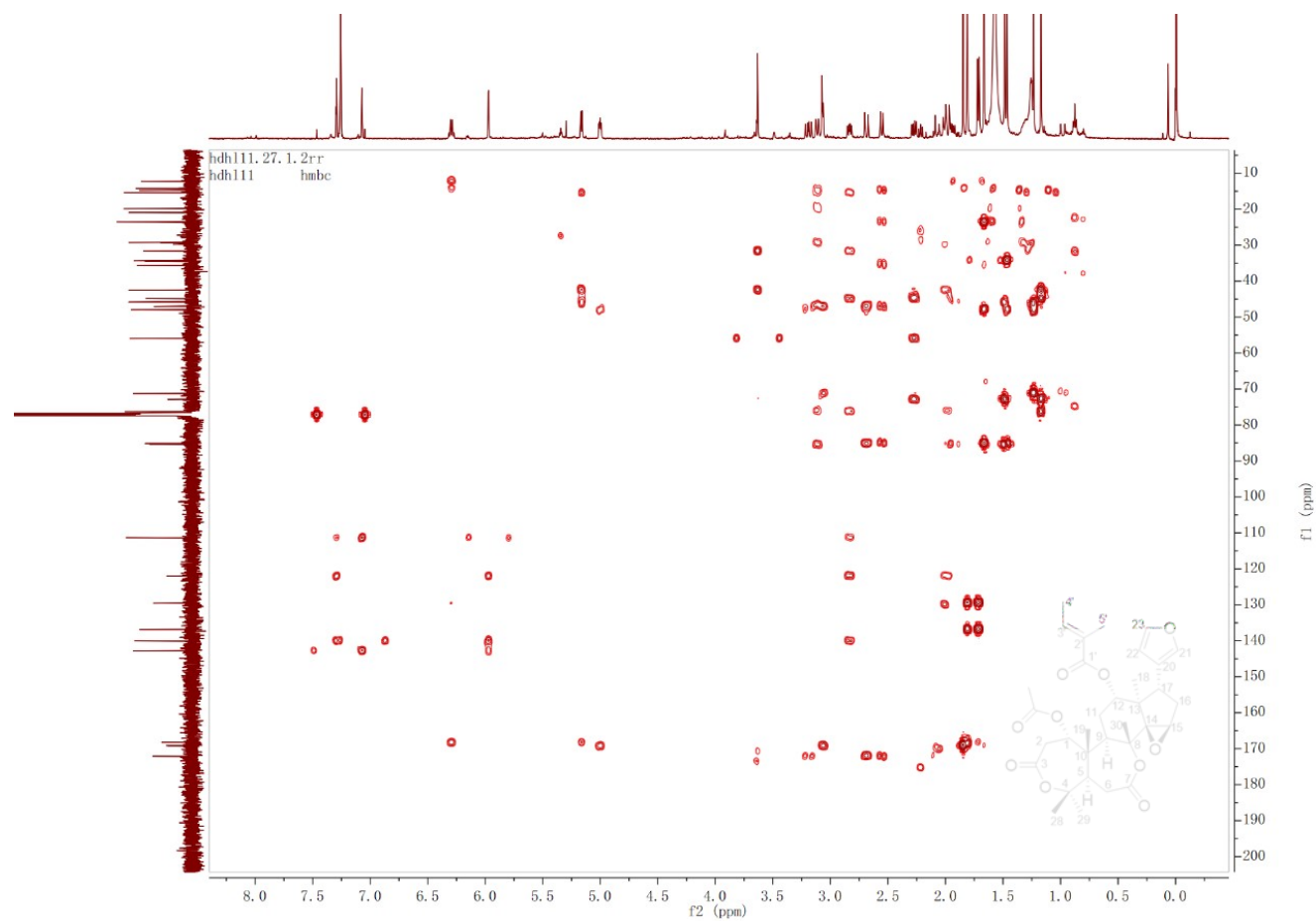


Figure S4. HMBC (600 MHz) spectrum of munronin V (1) in CDCl₃.

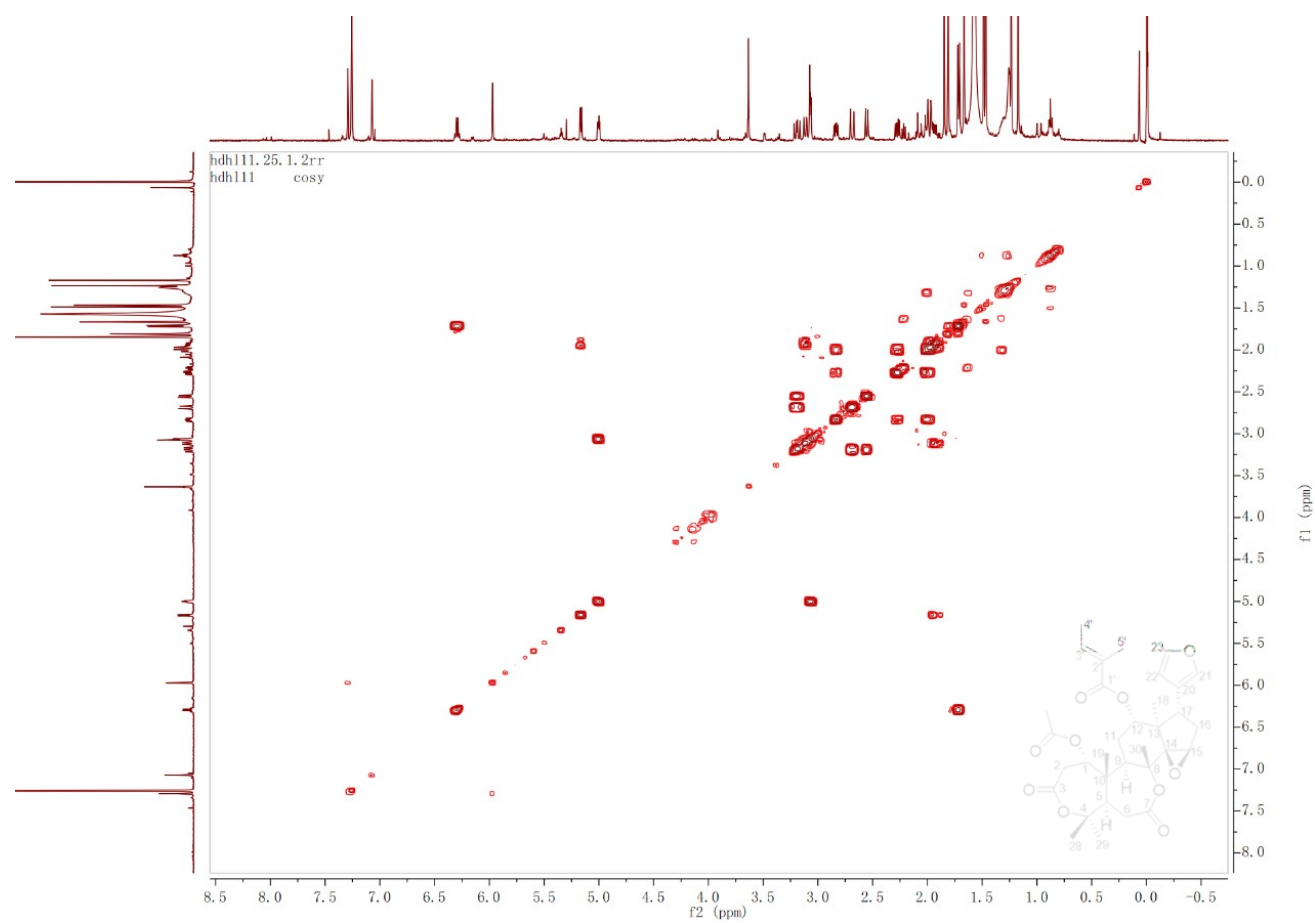


Figure S5. ^1H - ^1H COSY (600 MHz) spectrum of munronin V (1) in CDCl_3 .

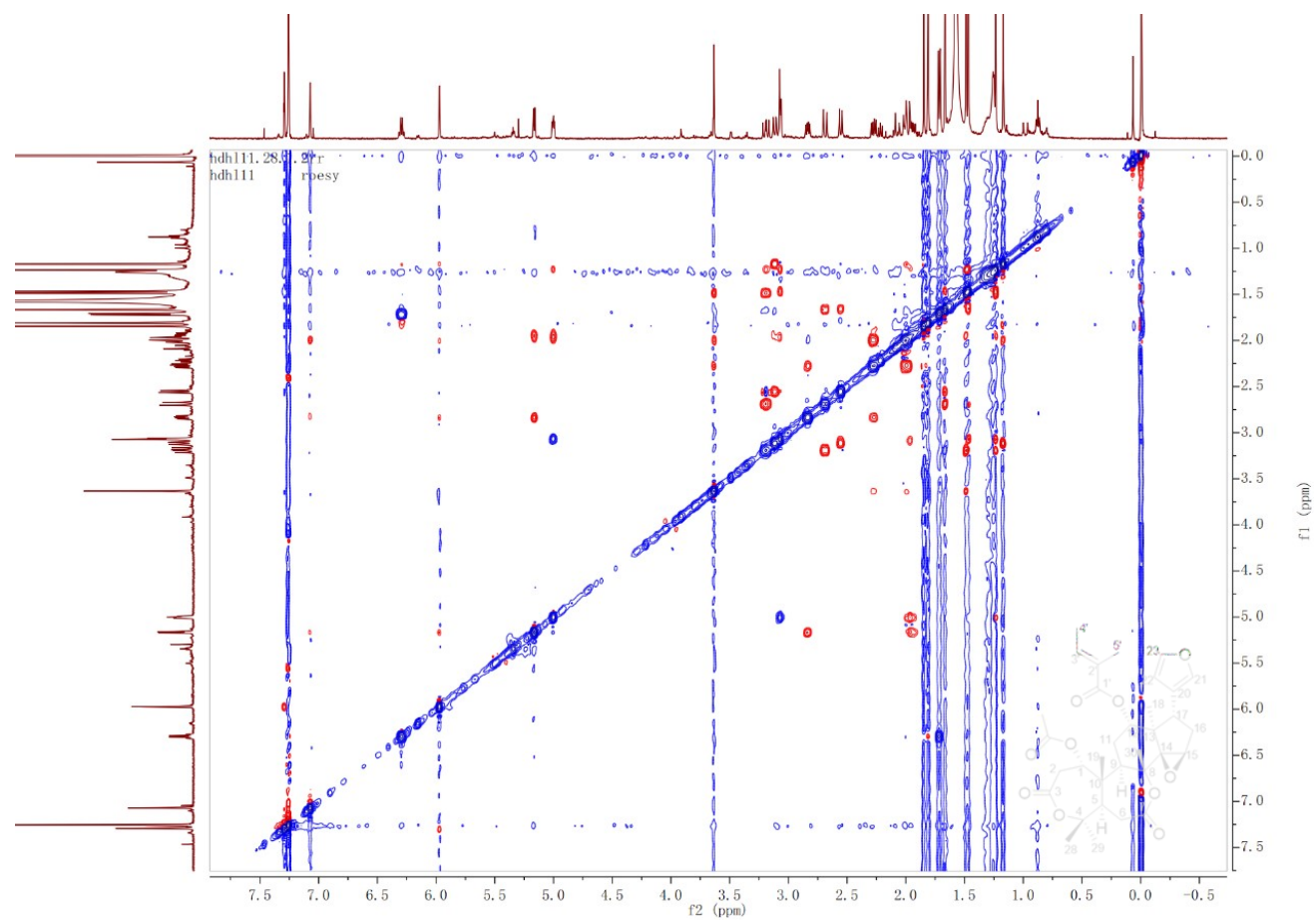


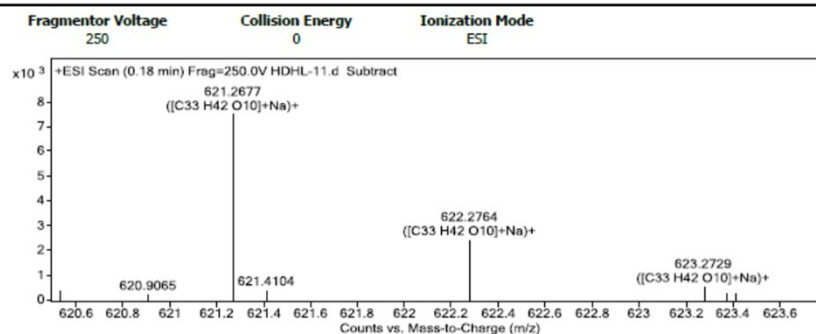
Figure S6. ROESY (600 MHz) spectrum of munronin V (1) in CDCl_3 .

Qualitative Analysis Report

Data Filename	HDHL-11.d	Sample Name	HDHL-11
Sample Type	Sample	Position	P1-A3
Instrument Name	Instrument 1	User Name	
Acq Method	s.m	Acquired Time	9/1/2020 2:47:52 PM
IRM Calibration Status	Success	DA Method	Default.m
Comment			

Sample Group		Info.
Acquisition SW	6200 series TOF/6500 series	
Version	Q-TOF B.05.01 (B5125.2)	

User Spectra



Peak List

m/z	z	Abund
256.2626	1	67156.39
274.2736	1	60743.55
300.2894	1	17320.86
318.2999	1	75757.48
340.2812	1	18160.7
353.2658	1	19327.06
362.3257	1	36945.31
437.1926	1	82691.19
438.1965	1	22311.29
653.2917	1	17143.64

Formula Calculator Element Limits

Element	Min	Max
C	3	60
H	0	120
O	0	30

Formula Calculator Results

Formula	CalculatedMass	CalculatedMz	Mz	Diff. (mDa)	Diff. (ppm)	DBE
C33 H42 O10	598.2778	621.2670	621.2677	-0.70	-1.13	13.0000

Figure S7. HRESIMS spectrum of munronin V (1).

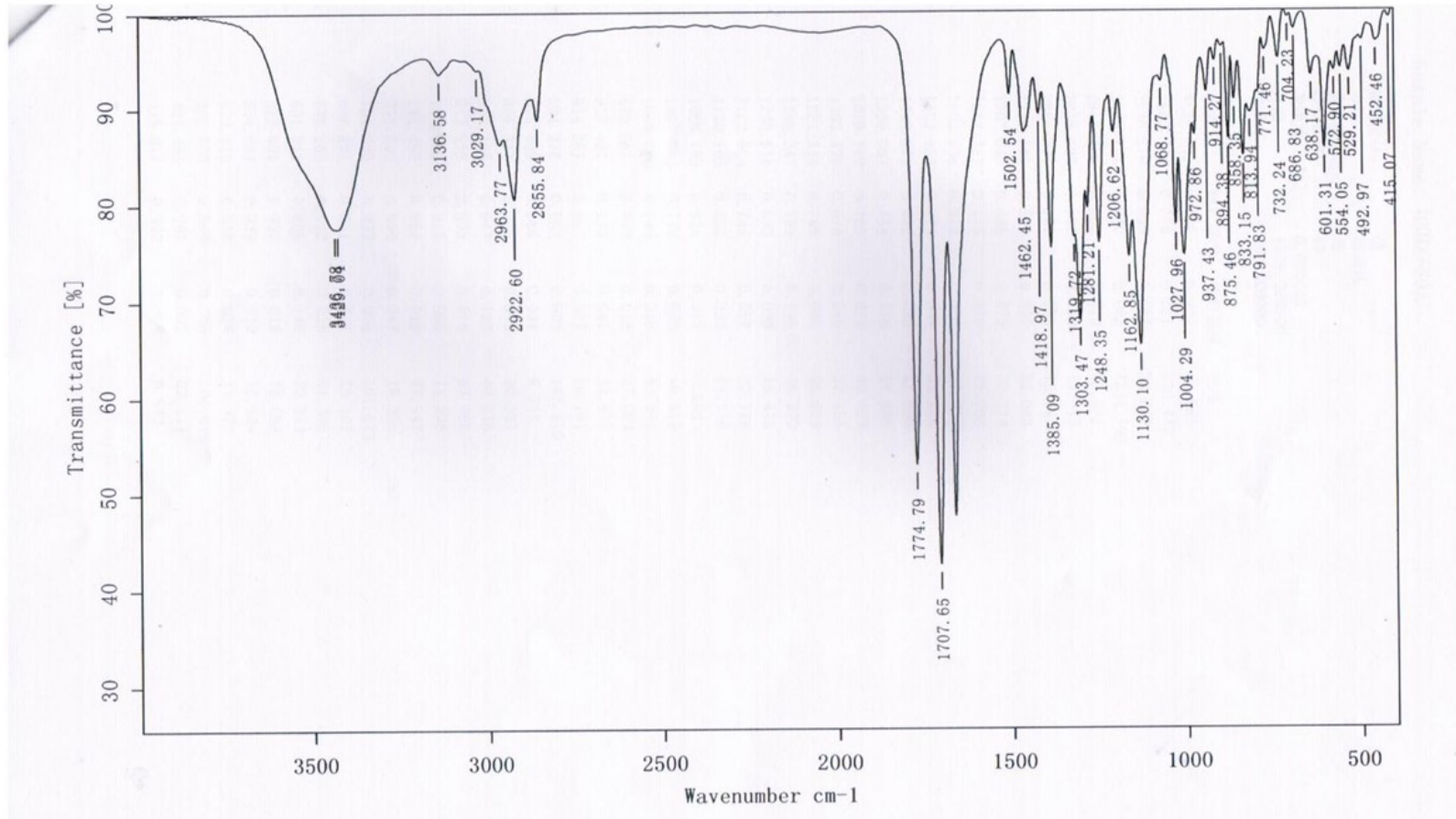


Figure S8. IR spectrum of munronin V (1).

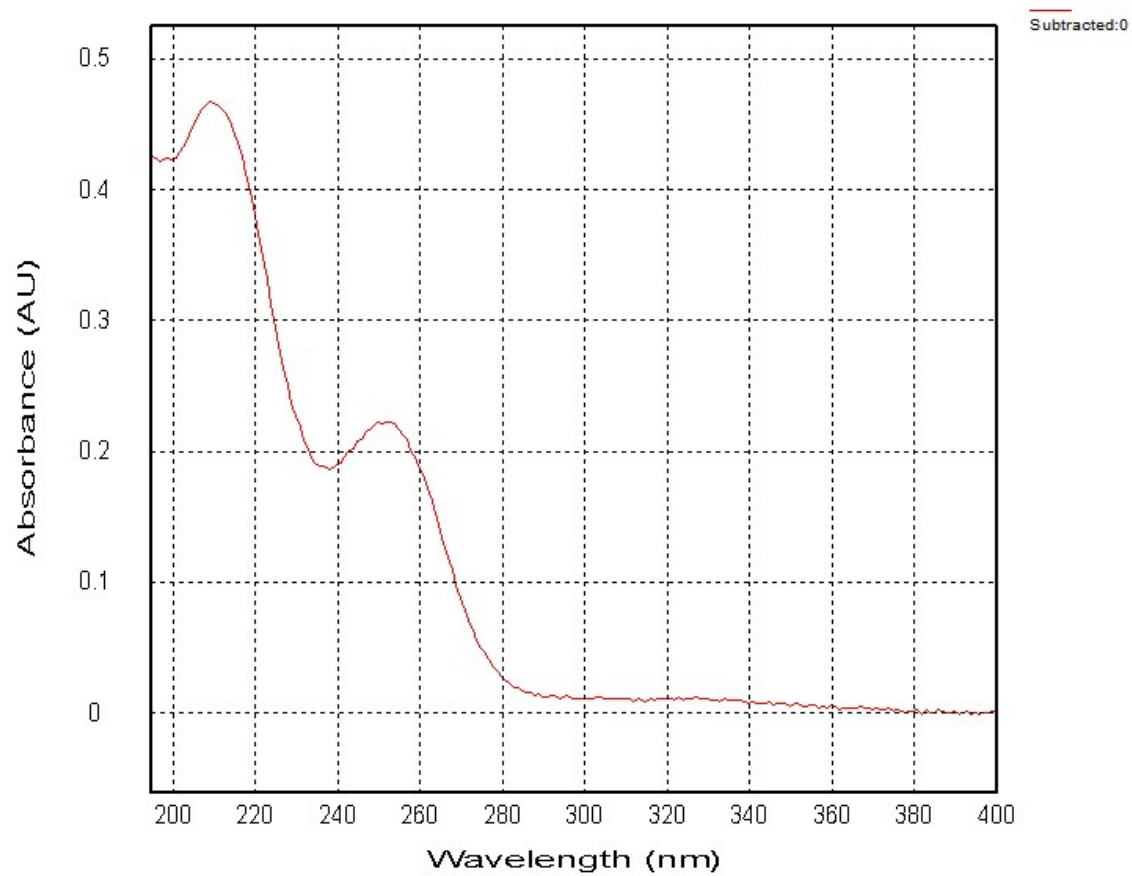


Figure S9. UV spectrum of munronin V (1).

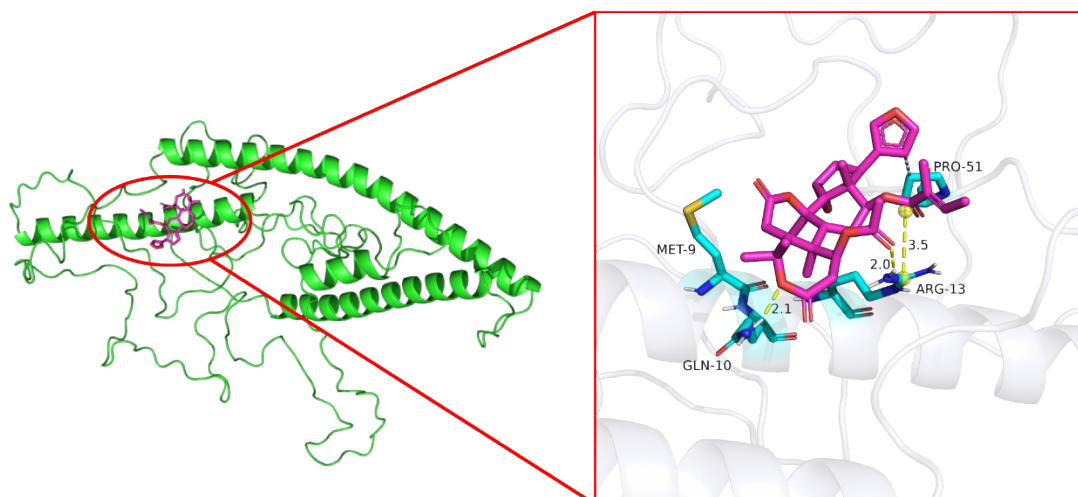


Figure S10. The molecular docking mode of munronin V (1) with TFEB.

The molecular docking experiment displayed that compound **1** could bind to the active site of TFEB in a proposed pose illustrated with predicted binding energy of -6.47 kcal/mol. Compound **1** forms hydrogen bonds with TFEB at GLN10 and ARG13, and forms hydrophobic interaction at MET9 and PRO51. These interactions would stabilize the binding of compound **1** with TFEB and potentially affect the activity of TFEB.

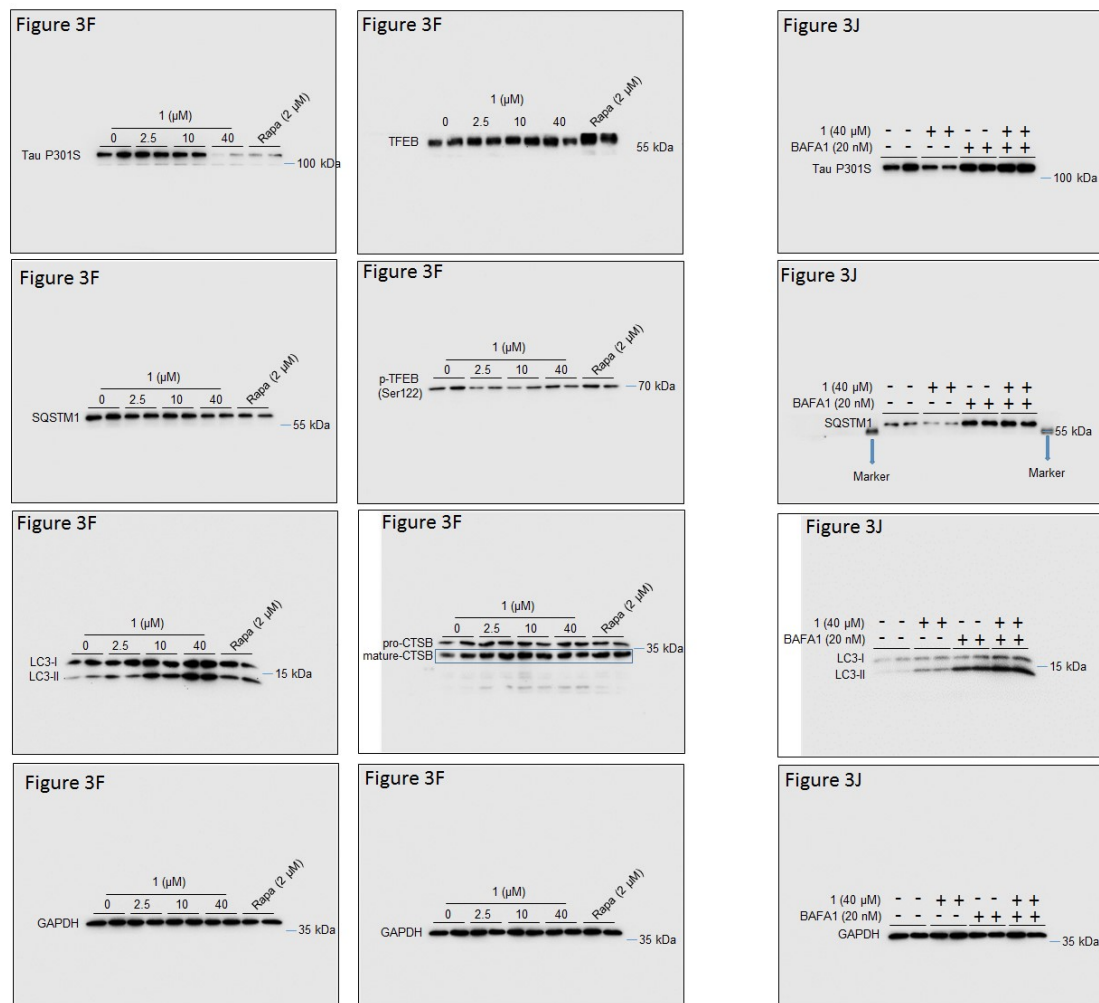


Figure S11. The raw images of the Western blot in Figure 3.

Reference

1. J. X. Song, Y. R. Sun, I. Peluso, Y. Zeng, X. Yu, J. H. Lu, Z. Xu, M. Z. Wang, L. F. Liu, Y. Y. Huang, L. L. Chen, S. S. Durairajan, H. J. Zhang, B. Zhou, H. Q. Zhang, A. Lu, A. Ballabio, D. L. Medina, Z. Guo and M. Li, *Autophagy*, 2016, **12**, 1372-1389.
2. Y. Xu, H. Ke, Y. Li, L. Xie, H. Su, J. Xie, J. Mo and W. Chen, *J Agric Food Chem*, 2021, **69**, 4663-4673.
3. R. Bi, W. Zhang, D. Yu, X. Li, H. Z. Wang, Q. X. Hu, C. Zhang, W. Lu, J. Ni, Y. Fang, T. Li and Y. G. Yao, *Neurobiology of aging*, 2015, **36**, 1604 e1607-1616.
4. X.-X. Pu, X.-Q. Ran, Y. Yan, Q.-Y. Lu, J.-C. Li, Y.-Y. Li, S.-P. Guan, M.-M. Cao, J. Liu, X.-J. Hao, R.-C. Luo and Y.-T. Di, *Phytochemistry Letters*, 2022, **50**, 141-146.
5. T. E. Hansen and T. Johansen, *BMC Biol*, 2011, **9**, 39.
6. X. H. Tang, R. C. Luo, M. S. Ye, H. Y. Tang, Y. L. Ma, Y. N. Chen, X. M. Wang, Q. Y. Lu, S. Liu, X. N. Li, Y. Yan, J. Yang, X. Q. Ran, X. Fang, Y. Zhou, Y. G. Yao, Y. T. Di and X. J. Hao, *Org*

Lett, 2021, **23**, 262-267.

7. R. Luo, Y. Fan, J. Yang, M. Ye, D. F. Zhang, K. Guo, X. Li, R. Bi, M. Xu, L. X. Yang, Y. Li, X. Ran, H. Y. Jiang, C. Zhang, L. Tan, N. Sheng and Y. G. Yao, *Signal Transduct Target Ther*, 2021, **6**, 325.
8. R. Luo, L. Y. Su, G. Li, J. Yang, Q. Liu, L. X. Yang, D. F. Zhang, H. Zhou, M. Xu, Y. Fan, J. Li and Y. G. Yao, *Autophagy*, 2020, **16**, 52-69.